2017 IEEE International Conference on Robotics and Automation (ICRA)
Singapore, May 29 - June 3, 2017

# HARMONIC POTENTIAL BASED COMMUNICATION-AWARE NAVIGATION and BEAMFORMING in CLUTTERED SPACES with FULL CHANNEL-STATE INFORMATION

Waqas Afzal and Ahmad A. Masoud

*Abstract*— **In this paper, we introduce a communication-aware algorithm to navigate mobile agents with non-trivial dynamics in cluttered environments. The navigation technique is based on the Harmonic Potential Field (HPF) approach to motion-planning. The proposed approach employs beamforming at the Base-Station (BS) simultaneously with the robot's motion to increase the Channel Spectral Efficiency (CSE). The approach is developed and basic proofs of performance are provided. Realistic simulations using the WINNER-II wireless channel model are used to demonstrate the navigation algorithm.**

## I. INTRODUCTION

Critical missions, such as search and rescue, reconnaissance, or surveillance, require autonomous agents to transmit real-time sensory data over a Wireless Communication Link (WCL). Therefore navigation systems for such agents are required to satisfy communication constraints so as to fulfill the data-transmission requirements. The core aspects that a communication-aware navigation systems needs to jointly tackle are [1], guidance, control, communication and energy consumption.

Recently, there has been a surge in interest in communication-aware navigation techniques. Researchers are looking at adapting the spatial movement of the agent so as to improve its Wireless Communication Channel (WCC). They are examining motion planning methods to jointly optimize sensing and communication performance along with spatial movements, [2], [3]. Moving in a formation among obstacles with Line Of Signt (LOS) constraint was presented in [4], while [5] introduced an indoor search while maintaining a communication link with an external BS. Another approach is to define the WCL in binary terms [6], i.e., connected or disconnected regions. All these techniques use simplistic representations of the wireless communication channel, assuming signal quality to be dependent on distance or based on LOS. Practically, in highly populated areas, or indoors, these simplified models, ignore the electromagnetic phenomena that affect the WCL.

Recent work has seen more realistic models of the WCC being used in motion planning. Lindhé [7] studied the improvement that can be gained by taking into account the effects of Multi-Path Components (MPC) on Received Signal Strength (RSS). The strategy tries to exploit the fact that the MPC of the transmitted signal constructively add at the Receiver (RX) within a few cm (function of wavelength). The core of the work looks at developing stop and go while tracking a reference trajectory based on the Signal to Noise Ratio (SNR) at the RX. Stopping intervals lengths were decided based on the SNR at the stopping point. Also, a probabilistic framework was developed to find the number of spatial stopping points around the original trajectory such that the agent is able to obtain the desired gain in SNR with a certain probability. Only Differential Drive Robots (DDR) and Front Steered Robots (FSR) type agents were studied. It was shown that these strategies could give up to $5dB$ of gain in SNR. The drawback of stop and go strategies is that discontinuous motion increases energy usage which deplete the battery energy reserve faster.

Mostofi in [8] introduced strategies to adapt the motion of a group of Unmanned Air Vehicles (UAV)s, cooperatively tracking a target with linear dynamics. The proposed work uses on-line SNR and correlation information of the WCL to help predict its information gain via communication and decide on its next movement. [9] introduces a communication-aware target sensing problem, where a group of autonomous agents locally sense the presence of targets and relay the sensed data to a BS. The WCC was modeled as a multi-scale random variable described probabilistically using underlying parameters that can be estimated based on previous observations. [10] developed a modified version of the navigation function to obtain path plans for tracking a mobile target and transmitting their estimated data (own location and location of target) to a BS.The connectivity was defined by comparing the SNR of the agent to a threshold and the regions where the SNR was below the threshold were modeled as obstacles and thus were integrated along with other physical obstacles in to the navigation function.

[11] builds on the work on estimation of the SNR field by estimating the underlying parameters of a multiscale (path loss, shadow fading and multipath fading) probabilistic model of the SNR. A communication aware plan for a holonomic agent was proposed based on minimizing the error in prediction of the SNR field. [12] proposes a communication-aware approach for multi-agent target tracking. The authors introduce a framework to estimate the underlying parameters for a multi-scale WCC model such that the mean squared error in channel assessment is minimized at the next step.

W. Afzal is with Department of Electrical Engineering, Control and Robotics, King Fahd University of Petroleum & Minerals, Dhahran, Saudi Arabia waqas@kfupm.edu.sa

A. A. Masoud is with Department of Electrical Engineering, Control and Robotics, King Fahd University of Petroleum & Minerals, Dhahran, Saudi Arabia masoud@kfupm.edu.sa

978-1-5090-4632-4/17/$31.00 ©2017 IEEE

Yuan et. al. in [13] examined the problem of maximizing the amount of information sent to a BS while moving on a fixed trajectory within a fixed time. It proposes modulation of the speed and transmission power at the agent during its motion along the trajectory to maximize the amount of data sent and minimize the energy consumption.

Most of the work found in the literature focuses on a specific aspect of Communication-Aware Navigation (CAN) while assuming simplistic models for the others. This can result in the actual performance significantly (sometime destructively) deviating from the desired one. Our focus is on developing a framework that is able to fuse together, in a provably-correct and energy efficient manner, the three critical aspects, wireless communication, guidance and control of an agent. At the heart of our work is the integration of wireless communication constraints with HPFs to obtain realizable goal-seeking guidance fields. The problem is introduced in Section II, followed by the description of the HPF based path-planning algorithm in Section III. We provide claims and proofs in Section IV followed by the results in Section VI and conclusions in Section VII.

## II. Problem Description & Formulation

We assume an agent equipped with a single antenna Transceiver (TRX) is moving with uniform velocity in a n-dimensional workspace $\mathcal{W}$ ($\mathcal{W} \in \mathbb{R}^n$) with a BS having $n_T$ antennas spaced half a wavelength apart. let $\mathbf{p}$ ($\mathbf{p} \in \mathcal{W}$) denote a position in the workspace . The WCC is assumed to be narrow band, reciprocal and Time-Division Duplex (TDD). Let the environment be stationary (WCC only changes with position). Assuming unit transmit power and no external interference at the agent, the SNR of the WCL, is given by

$$\gamma = \frac{S}{N} = \frac{\mathbf{h}\mathbf{h}^H}{\sigma^2} \tag{1}$$

Where $\mathbf{h} \in \mathbb{C}^{n_T \times 1}$ is the complex scalar channel gain of the WCL. $\sigma^2$ is the variance of zero mean Additive White Gaussian Noise (AWGN) at the receiver. The data-transmission efficiency of such a WCL can be quantified using CSE [14]. CSE of a WCL is directly dependent on its SNR and is given by

$$\eta(\mathbf{h}) = \log_2\left(1 + \gamma(\mathbf{h})\right)(bits/s/Hz) \tag{2}$$

The total data that can be reliably transmitted at a particular location depends on the time spent by the receiver (the agent) at a particular location. Ideally, it would be desired that the agent spends more time in regions with higher CSE. The time an agent spends at a particular location along its trajectory is nothing but the inverse of the magnitude of the velocity at that location . This leads us to the following definition

*DEFINITION 1:* Let $\beta : \mathcal{W} \to \mathbb{R}_+$, be a function that maps each point in the workspace to a scalar positive real number equal to the maximum possible data that can be reliably transmitted at that point. Then, let $\beta$ be defined as the Data-Flow Efficiency (DFE) of a point in the workspace and $\beta(\mathbf{p})$ is a scalar field defined by,

$$\beta(\mathbf{p}) = \frac{\eta}{|\dot{\mathbf{p}}|} \quad (bits/m/Hz) \tag{3}$$

Def. 1 is important in the sense that it gives a measure of the communication performance based on the kinematic properties of the agent. It is a ratio of SNR to velocity magnitude, thus, linking the position and time spent at a position with its SNR. It gauges the amount of data that can be sent per spatial point in the trajectory. It should also be noted that the DFE can easily be generalized for broad band channels and time varying environments.In the rest of the work we will use the SNR and CSE interchangeably as they are monotonically related. Let the start position be $\mathbf{p}_S$, and the goal position be $\mathbf{p}_G$. let the Hard Obstacle or Hazardous Region (HO) (regions of arbitrary geometry where the agent can get damaged) be denoted by $\mathcal{O}$ and the Dead Communication Zones (DCZ), $\mathcal{O}_{DCZ}$, be defined as

*DEFINITION 2:* DCZ, $\mathcal{O}_{DCZ}$, are regions where the SNR goes below a threshold such that CSE becomes prohibitively low. .

$$\mathcal{O}_{DCZ} = \{\mathbf{p} \in \mathcal{W}_a | \gamma(\mathbf{p}) \leq \epsilon_D, \epsilon_D \to 0\}, \epsilon_D \in \mathbb{R} \tag{4}$$

where,

$$\mathcal{O}_{DCZ} \subset \mathcal{W}_a = \bigcup_{i=1}^{N_{DCZ}} o_{dcz_i}$$

where $N_{O_c}$ is the number of DCZ in the workspace.
Assuming single integrator dynamics for the agent and letting the complete knowledge of the SNR and HO be available to the agent, the problem can then be formulated as,

$$\begin{aligned}
&\textbf{for} \\
&\dot{\mathbf{p}} = u \\
&\text{find} \\
&\mathbf{u}(\mathbf{p}, \mathbf{p}_G, \mathbf{p}_S, \gamma, \mathcal{O}) \\
&\text{Such that,} \\
&\mathbf{p}(0) = \mathbf{p}_S \\
&\lim_{t\to\infty} \mathbf{p}(t) \to \mathbf{p}_G \\
&\mathbf{p}(t) \bigcap \mathcal{O}_{DCZ} \equiv \phi, \ \forall t \\
&\mathbf{p}(t) \bigcap \mathcal{O} = \phi, \ \forall t \\
&\mathbf{p}(t) \in \mathcal{T} \mid \boldsymbol{\Upsilon}(\mathbf{p}(t)) \leq \boldsymbol{\Upsilon}(\mathbf{q}_i), \mathbf{q}_i \in \mathcal{T}, \ \forall i = 1, 2, \cdots, \infty
\end{aligned} \tag{5}$$

Where $\boldsymbol{\Upsilon}$ is the functional that should be minimized by the trajectory realized and $\mathcal{T}$ is the set of all possible trajectories of the agent.

## III. Model-Based Communication-Aware Navigation (MBCAN)

In this work, we assume that the complete SNR knowledge of the environment is available to the agent. We build on the Gamma-Harmonic Potential Field (GHPF) planner in [15] to generate trajectories that satisfy eq. 5. Results are derived for an agent with single integrator dynamics and extended in a provably correct way for realistic non-holonomic agents using the Virtual Velocity Attractor (VVA)

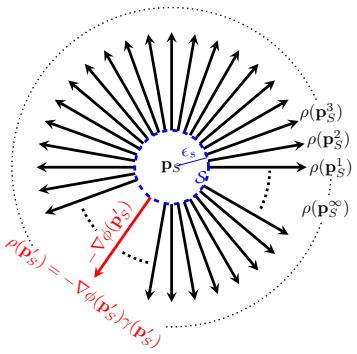


Fig. 1: Different values of $\rho$ at different points on $\mathcal{S}$ which is a circle in a 2D workspace

approach presented in [16]. Let $\mathcal{O} \in \mathbb{F}_2$ be a scalar binary field representing the HO in the workspace. $\mathcal{O}$ is 1 for regions where obstacles are present and 0 otherwise. Let $\mathbf{\Gamma}_\mathcal{W}$ represent the boundary of the workspace and $\mathbf{\Gamma}_\mathcal{O}$ be the boundary of all the HO in the workspace. Finally, let $\phi(\mathbf{p})$ be a scalar Potential Field (PF) at each point in the workspace.

Generating a communication-aware path begins by solving the Partial Differential Equation (PDE) as shown below

$$\begin{aligned} &\textbf{solve} && \nabla(\gamma(\mathbf{p})\nabla\phi(\mathbf{p})) = 0,\ \mathbf{p} \in \mathcal{W} \\ &\textbf{s. t.} && \phi(\mathbf{p}_S) = 1,\ \phi(\mathbf{p}_G) = 0 \\ & && \frac{\partial\phi}{\partial\mathbf{n}} = 0,\ \text{at } \mathbf{p} \in \mathbf{\Gamma}_\mathcal{W}, \mathbf{p} \in \mathbf{\Gamma}_\mathcal{O} \end{aligned} \tag{6}$$

Then a sphere $\mathcal{S}$ of arbitrarily small radius is defined around $\mathbf{p}_S$ as shown in figure 1

$$\mathcal{S} = \{\mathbf{p} \,|\, |\mathbf{p} - \mathbf{p}_S| = \epsilon_s\}, 0 < \epsilon_s \ll 1 \tag{7}$$

A point $\mathbf{p}'_S \in \mathcal{S}$ is selected such that

$$\rho(\mathbf{p}'_S) \geq \rho(\mathbf{p}_S^i \in \mathcal{S}), i = 1, 2, \cdots, \infty \tag{8}$$

where $\rho$, is defined as

$$\rho(\mathbf{p}) = -\nabla\phi(\mathbf{p})\gamma(\mathbf{p}) \tag{9}$$

Finally, the path is generated using the following gradient dynamical system.

$$\dot{\mathbf{p}} = -\nabla\phi(\mathbf{p}),\ \mathbf{p}(0) = \mathbf{p}'_S \tag{10}$$

The MBCAN algorithm is given in algorithm 1.

## IV. Analysis

Let the communication-aware 'effort' be defined as:

$$\gamma\,|\nabla\phi|^2 \tag{11}$$

$\gamma$ at a point can be increased by increasing the transmission power. The path-planner can only affect the velocity of the agent. Thus, eq. 11 captures both the data-transmission and motion energy of the agent at a point. Note that the Boundary

**Algorithm 1** MBCAN

1: Get Workspace $\mathcal{W}$.
2: Get SNR representation $\gamma(\mathbf{p})$ for $\mathcal{W}$.
3: Get HO representation $\mathcal{O}(\mathbf{p})$ for $\mathcal{W}$.
4: Get start position $\mathbf{p}_S$ of agent.
5: Get goal position $\mathbf{p}_G$.
6: GHPF($\mathcal{W}$,$\eta$,$\mathcal{O}$,$\mathbf{p}_S$,$\mathbf{p}_G$). ▷ Calling function GHPF
7: Find $\mathbf{p}'_S$ using eq. 8
8: Solve $\dot{\mathbf{p}} = \int_0^\infty -\nabla\phi dt,\ \mathbf{p}(0) = \mathbf{p}'_S$ for $\mathbf{p}(t)$.
9: **function** GHPF($\mathcal{W}$,$\gamma$,$\mathcal{O}$,$\mathbf{p}_S$,$\mathbf{p}_G$)
10: Set $\dfrac{\partial\phi}{\partial n} = 0$ at $\mathbf{\Gamma}_\mathcal{W}$.
11: Set $\dfrac{\partial\phi}{\partial n} = 0$ at $\mathbf{\Gamma}_\mathcal{O}$.
12: Set $\phi(\mathbf{p}_S) = 1$.
13: Set $\phi(\mathbf{p}_G) = 0$.
14: Solve $\nabla \cdot (\gamma\nabla\phi) = 0$ for $\phi$.
15: **return** $\phi$.
16: **end function**

Value Problem (BVP) eq. 6 minimizes the Dirichlet Integral [17], which has eq. 11 as its integrand.

$$\int_{\mathcal{W}_\phi} \gamma\,|\nabla\phi|^2\, d\mathcal{W}_\phi = \sum_{i=1}^{\infty} \int_{\mathbf{p}_S}^{\mathbf{p}_G} \gamma\,|\nabla\phi|^2\, dq_i \tag{12}$$

Since the agent can choose from infinitely many trajectories, $\mathbf{q}_i, i = 1, 2, \cdots, \infty$, as shown in figure 2 eq. 12 is a sum

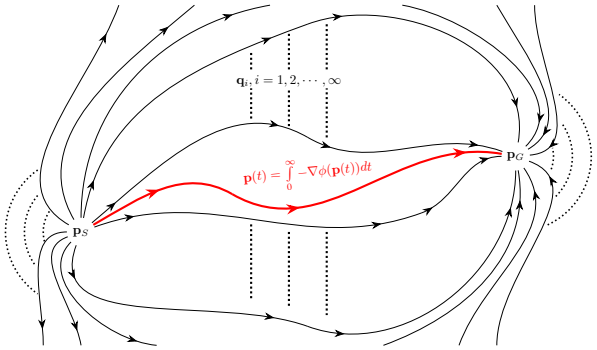


Fig. 2: Infinitely possible trajectories

of line integrals that accumulate eq. 11 over each trajectory $\mathbf{q}_i$. Any increase in path length of a trajectory will increase the line integral value. Moreover locally at each point on the trajectory if the SNR is high, eq. 11 can only be minimized if $|\nabla\phi|$ is minimized. Thus, minimization of eq. 12 will assign the shorted possible trajectories to regions with high $\gamma$.

In the following, we provide our propositions and their proofs.

*PROPOSITION 1:* The magnitude of $\rho$, defined in eq. 9 is constant along the trajectory described by eq. 10 and is equal to $|\rho(\mathbf{p}'_S)|$. Where, $\phi$ is obtained as a solution to eq. 6

*Proof:* It can be noted that eq. 6 implies that the divergence of the term

$$\gamma(\mathbf{p})\nabla\phi(\mathbf{p}), \mathbf{p} \in \mathcal{W}_\phi \tag{13}$$

is zero. In other words continuity of the product in eq. 13 is imposed locally at each point in $\phi$. But the product in eq. 13 is represented by $\rho(\mathbf{p})$ as described in eq. 9. Therefore, $|\rho(\mathbf{p}(t))|$ will be constant for all $t$ and since the starting point is chosen as $\mathbf{p}'_S$ (eq. 8), it can be concluded that

$$|\rho(\mathbf{p}(t))| = constant = |\rho(\mathbf{p}'_S)| \qquad \blacksquare$$

*DEFINITION 3:* Let $\mathcal{T}$ be a set of infinitely possible trajectories, $\mathbf{q}_i \in \mathcal{T}, i = 1, 2, 3, \cdots, \infty$, an agent can take from its starting position, $\mathbf{p}_S \in \mathcal{W}_\phi$, to a goal position, $\mathbf{p}_G \in \mathcal{W}_\phi$, in its workspace as shown in figure 2. A trajectory $\mathbf{q}_i$ can be realized by choosing a starting orientation $\delta_i$ by selecting a point on $\mathcal{S}$ (defined in eq. 7) then following the gradient of $\phi$ at each point in the PF. Since the PF obtained as a solution to (6) is conservative [18], using the fundamental theorem of calculus, the line integral over any trajectory $\mathbf{q}_i$ will be given by

$$\int_{\mathbf{p}_S=\mathbf{q}_i(0)}^{\mathbf{p}_G=\mathbf{q}_i(\infty)} -\nabla\phi(\mathbf{q}_i) \cdot d\vec{\mathbf{q}}_i = \phi(\mathbf{p}_S) - \phi(\mathbf{p}_G) = 1 \qquad (14)$$

Using eq. 9, eq. 14 can be written as

$$1 = \int_{\mathbf{p}_S}^{\mathbf{p}_G} \frac{\rho(\mathbf{q}_i)}{\gamma(\mathbf{q}_i)} \cdot d\vec{\mathbf{q}}_i \qquad (15)$$

where $\rho$ at the starting position can be written as

$$\rho_i = \rho(\mathbf{p}^i_S) = \left|\rho(\mathbf{p}^i_S)\right| \frac{\delta_i}{|\delta_i|} \qquad (16)$$

Similarly at the starting position, $d\mathbf{q}_i$ can be written as

$$d\vec{\mathbf{q}}_i = |\dot{q}_i| \frac{\delta_i}{|\delta_i|} dt \qquad (17)$$

Once a starting orientation is chosen by the agent, the factor $\frac{\delta_i}{|\delta_i|}$ in equations 16 and 17 will be replaced by $\frac{\nabla\phi}{|\nabla\phi|}$. Using eq. 16 and eq. 17 in eq. 15 we get

$$1 = \int_0^\infty \frac{|\rho_i| \frac{\delta_i}{|\delta_i|}}{\gamma} \cdot |\dot{q}_i| \frac{\delta_i}{|\delta_i|} dt = \int_0^\infty \frac{|\rho_i| \, |\dot{q}_i|}{\gamma} dt \qquad (18)$$

From proposition 1

$$|\rho(\mathbf{q}_i(t))| = constant, \forall t$$

This leads us to the definition of a functional, $\boldsymbol{\Upsilon}$, that returns a scalar for any trajectory taken by the agent

$$\boldsymbol{\Upsilon}(\mathbf{q}_i(t)) = \frac{1}{|\rho_i|} = \int_0^\infty \frac{|\dot{\mathbf{q}}_i|}{\eta} dt = \int_0^\infty \frac{1}{\beta(\mathbf{q}_i(t))} dt, i = 1, \cdots, \infty \qquad (19)$$

where $\beta$ is the DFE (def. 1).

*PROPOSITION 2:* The trajectory $\mathbf{p}(t)$ obtained from the gradient dynamical system in eq. 10.

$$\dot{\mathbf{p}} = -\nabla\phi(\mathbf{p}), \ \mathbf{p}(0) = \mathbf{p}'_S \in \mathcal{W}_\phi$$

where $\phi$ is obtained as a solution to eq. 6 minimizes the functional, $\boldsymbol{\Upsilon}$ defined in eq. 19, where the trajectory $\mathbf{p}(t)$ is parameterized by time.

*Proof:* Since the starting orientation of the trajectory obtained using eq. 10 for the HPF generated by eq. 6, is chosen to be such that $\rho$ (eq. 9) is maximum at that orientation (eq. 8). Thus from the definition of $\boldsymbol{\Upsilon}$ (eq. 19), it will be the minimum of all possible trajectories $\mathbf{q}_i$. $\blacksquare$

It should be noted that eq. 8 is a direct consequence of propostions 1 and 2.

The proofs for DCZ and HO avoidance can be found in [19].

## V. Joint Motion And Beamforming

Typically, in the wireless communication literature, the user (robot in our case) is considered to have a fixed position while beamforming is applied at the BS [20]. This is valid for slow moving robots but for high speed agents, this could lead to the beam being formed for positions that are no longer occupied by the robot. Also, the future spatial positions of the user are not known in traditional beamforming problems. Using the MBCAN, the robot computes its position as a continuous trajectory, $\mathbf{p}(t)$, to the goal. This spatial information of the robot can be used to predict the WCC, $\mathbf{h}(t)$ along the trajectory [9]. Thus, a complex vector trajectory $\mathbf{w}(t)$ can then be simultaneously computed to improve the SNR along the trajectory of the agent.

Zero-Forcing (ZF) beamforming is known to give near system capacity performance if the WCC is known [21]. Based on the predicted WCC, $\mathbf{h}(t)$, for the robot path, $\mathbf{p}(t)$, we propose a ZF beamforming frame work as follows

$$\mathbf{w}(t) = \frac{\mathbf{h}(t)(\mathbf{h}(t)^H \mathbf{h}(t))^{-1}}{\|\mathbf{h}(t)(\mathbf{h}(t)^H \mathbf{h}(t))^{-1}\|_2} \qquad (20)$$

where $\|\mathbf{w}(t) \in \mathbb{C}^{n_T \times 1}\|_2 = 1, \forall t$. The agent is equipped with a single antenna and beamforming is only employed at the BS. This is due to the reason that adding multiple antennas requires an increase in the agent size. It also increases energy consumption. Since we assume reciprocity in the WCC in uplink and downlink, techniques like maximal ratio combining can be used to obtain a similar gain at the BS for data transmitted by the single antenna agent to the BS.

## VI. Simulation Results

For the simulation, a 2-D $10m \times 10m$ workspace was assumed with a BS ($n_T = 4$) located at $(5, 0)$. The WCC gain $\mathbf{h}$ was obtained by using the WINNER II channel models [22] for an indoor environment (frequency 2.5GHz). SNR at each point was computed using eq. 1 (with $\sigma^2 = 1$).

Figure 3 shows the Communication-Aware Trajectory (CAT) (red color) obtained using MBCAN superimposed on the SNR and HO (blue color) representation in a cluttered environment. The Communication-Blind Trajectory (CBT) is obtained using HPF without SNR information. It can be seen that the CAT avoids possible DCZ due to the shadowing caused by the obstacles. It avoids all the HO and maintains

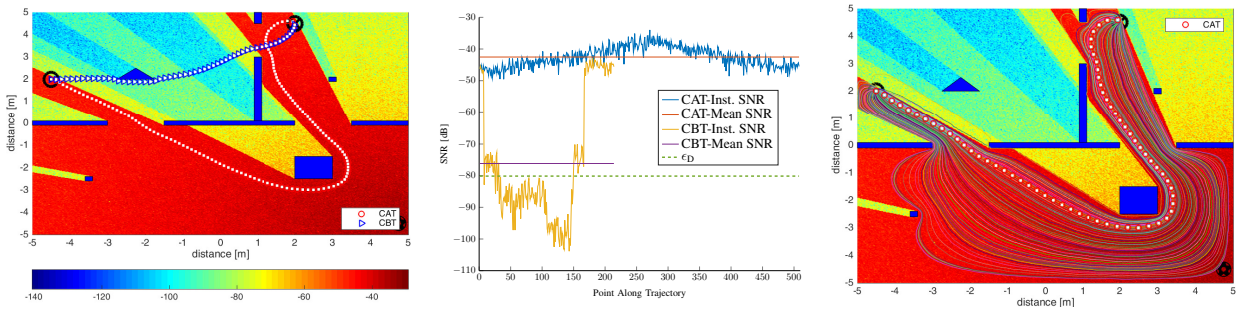


Fig. 3: HPF based SNR-aware and -unaware trajectories in a complex environment

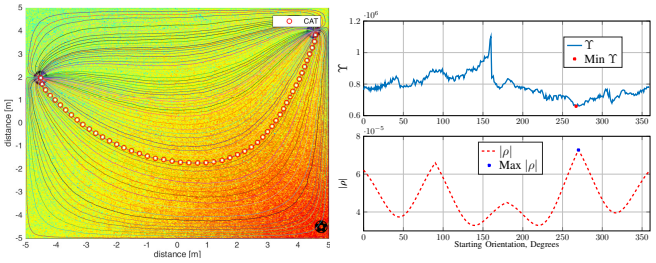


Fig. 4: Magnitude of $\rho$ at different points on $\mathcal{S}$ and functional $\boldsymbol{\Upsilon}$ due to the resulting trajectories.

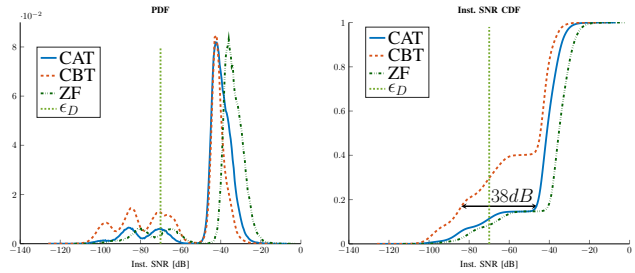


Fig. 5: PDF and CDF of instantaneous SNR at each point along the trajectory

a safe distance from the HO. It can be seen that without any SNR knowledge, the agent is still able to reach the goal and avoid the HO.The second figure shows the SNR at each instant along the CAT and its mean are compared to when the agent moves without any knowledge of the SNR. The third figure shows trajectories obtained by choosing different points on the starting circle $\mathcal{S}$. It can be seen that all the trajectories avoid the DCZ and HO. Thus if an agent is bumped off course of the original trajectory, it would still be able to navigate towards the goal while avoiding the DCZ and HO.

Figure 4 shows CAT in an empty environment with a BS obtained by choosing different starting points on $\mathcal{S}$ as defined in eq. 7. The corresponding magnitude of $\rho$ (eq. 9) and the functional $\boldsymbol{\Upsilon}$ ()eq. 19 are) are plotted in the second figure. It can be seen that the maximum value of $\rho$ corresponds to the minimum value of the $\boldsymbol{\Upsilon}$. Figure 5 compares the Probability Density Function (PDF) and Cumulative Distribution Function (CDF) of the instantaneous SNR and ZF beam-forming at each instant along the trajectory of the CATs with trajectories that have no SNR knowledge. The PDF was obtained by generating 4000 trajectories in the cluttered environment (Figure 3), using random start and goal position for each trajectory sample. It can be seen that the PDF of the CAT, has a higher concentration at higher SNRs. A more clear picture can be seen in CDF, where it can be seen that the CATs significantly improves the SNR especially lower SNR values. This is mainly due to the avoidance of shadowed regions using MBCAN. The difference is very small for trajectories that are in high SNR regions compared to low SNR regions. At high SNRs the performance of both blind and communication aware

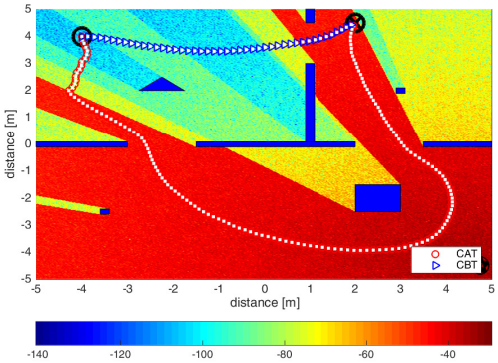


Fig. 6: Path for starting position in a DCZ

trajectories start to converge. It can also be seen that with joint simultaneous ZF beamforming and MBCAN, there is a further gain in the the instantaneous SNR of the CAT in the whole SNR range. Finally, it can be seen that nearly $30\%$ of the instantaneous SNR of the CBT lie in a DCZ. However, nearly $12\%$ of instantaneous SNR for CAT and $9\%$ for joint ZF and MBCAN trajectories also lie in DCZs. This can be explained by the scenario when $\mathbf{p}_S$ and $\mathbf{p}_G$ lie in a DCZ and the robot has to move within the DCZ until it enters higher SNR regions.

Figure 6 shows the trajectory obtained using MBCAN when the starting position of the agent is in a DCZ. The SNR (figure 7) is below the DCZ threshold $\epsilon_D$ (dashed green line in the SNR plot) at the starting position but crosses $\epsilon_D$ and remains above it until the path ends at the goal position. It can be seen that the there is no random motion and the path exit obtained initially exits the DCZ towards a region

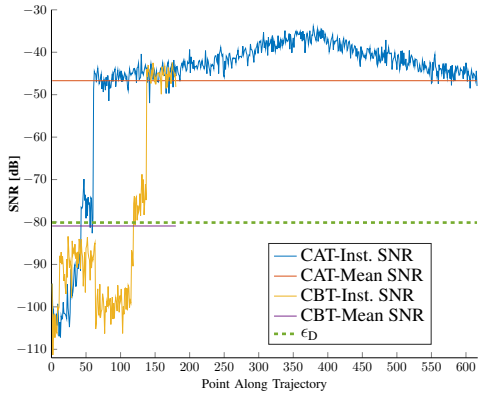


Fig. 7: SNR for trajectories in figure 6

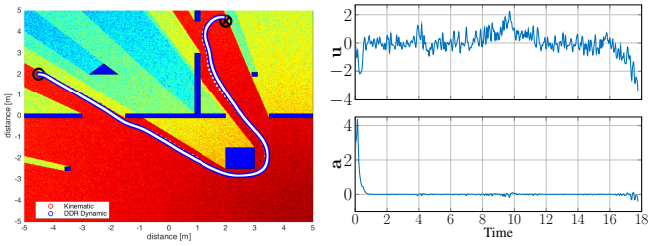


Fig. 8: Dynamic Trajectory and Control Signals of a DDR

with a better SNR and then moves towards the goal. The trajectories obtained using eq. 10 for a $\phi$ can be realized for a large class of agents using the VVA approach presented in [16]. The trajectory of a DDR described by

$$[\dot{x}, \dot{y}, \dot{\theta}, \dot{v}]^T = [v\cos\theta, v\sin\theta, u, a]^T \qquad (21)$$

is shown in figure 8 for the cluttered environment above.

## VII. Conclusion

This paper suggests a provably-correct, communication aware navigation control system. The system can safely steer an agent to a target zone while maintaining a good WCL with a base station. The suggested procedure was able to avoid shadow fades in cluttered environments. It significantly improves the mean SNR along the trajectory. This paper tackles the case where the SNR map is fully known. The results obtained with this method will serve as the benchmark for other methods with more realistic assumptions on SNR knowledge. This method can be extended to generate the navigation control signal based on on-line sensory-based measurement of the signal strength and obstacle fields. Elementary results regarding the extension of this method to the sensor-based case where the agent has no prior knowledge ot he SNR are quite promising and will be published in future works. We are currently working on developing the theoretical framework for this case along with the necessary proofs.

## Acknowledgment

The authors acknowledge the assistance of King Fahd University of Petroleum and Minerals and the high performance computing resources provided by KFUPM that contributed to the research results reported within this paper.

## References

[1] R. R. Murphy, S. Tadokoro, D. Nardi, A. Jacoff, P. Fiorini, H. Choset, and A. M. Erkmen, "Search and rescue robotics," in *Springer Handb. Robot.*, O. Siciliano, Bruno and Khatib, Ed. Springer Berlin Heidelberg, 2008, pp. 1151–1173.

[2] T. Chung, J. Burdick, and R. Murray, "A decentralized motion coordination strategy for dynamic target tracking," in *Proc. 2006 IEEE Int. Conf. Robot. Autom. 2006. ICRA 2006.* Orlando, FL: IEEE, 2006, pp. 2416–2422.

[3] P. Yang, R. A. Freeman, and K. M. Lynch, "Distributed cooperative active sensing using consensus filters," in *Proc. 2007 IEEE Int. Conf. Robot. Autom.* IEEE, Apr. 2007, pp. 405–410.

[4] J. Esposito and T. Dunbar, "Maintaining wireless connectivity constraints for swarms in the presence of obstacles," in *Proc. 2006 IEEE Int. Conf. Robot. Autom. 2006. ICRA 2006.* Orlando, FL: IEEE, 2006, pp. 946–951.

[5] R. Arkin and J. Diaz, "Line-of-sight constrained exploration for reactive multiagent robotic teams," in *7th Int. Work. Adv. Motion Control. Proc. (Cat. No.02TH8623).* IEEE, 2002, pp. 455–461.

[6] Z. Butler and D. Rus, "Event-based motion control for mobile-sensor networks," *IEEE Pervasive Comput.*, vol. 2, no. 4, pp. 34–42, Oct. 2003.

[7] M. M. LINDHÉ, "Communication-aware motion planning for mobile robots," PhD Dissertation, KTH, Stockholm, 2012.

[8] Y. Mostofi, "Decentralized communication-aware motion planning in mobile networks: An information-gain approach," *J. Intell. Robot. Syst.*, vol. 56, no. 1-2, pp. 233–256, May 2009.

[9] A. Ghaffarkhah and Y. Mostofi, "Dynamic networked coverage of time-varying environments in the presence of fading communication channels," *ACM Trans. Sens. Networks*, vol. 10, no. 3, pp. 1–38, Apr. 2014.

[10] ——, "Communication-aware target tracking using navigation functions centralized case," in *Proc. 2nd Int. Conf. Robot. Commun. Coord.* Odense: IEEE, 2009.

[11] ——, "Channel learning and communication-aware motion planning in mobile networks," in *Proc. 2010 Am. Control Conf.* Baltimore, MD: IEEE, Jun. 2010, pp. 5413–5420.

[12] ——, "Communication-aware motion planning in mobile networks," *IEEE Trans. Automat. Contr.*, vol. 56, no. 10, pp. 2478–2485, Oct. 2011.

[13] Y. Yan and Y. Mostofi, "Co-optimization of communication and motion planning of a robotic operation under resource constraints and in fading environments," *IEEE Trans. Wirel. Commun.*, vol. 12, no. 4, pp. 1562–1572, Apr. 2013.

[14] A. F. Molisch, *WIRELESS COMMUNICATIONS*, 2nd ed. Wiley, 2010.

[15] A. A. Masoud, "Motion planning with gamma-harmonic potential fields," *IEEE Trans. Aerosp. Electron. Syst.*, vol. 48, no. October 2012, pp. 2786–2801, 2012.

[16] ——, "A virtual velocity attractor, harmonic potential approach for joint planning and control of a uav," in *Proc. 2011 Am. Control Conf.* San Francisco, CA: IEEE, Jun. 2011, pp. 432–437.

[17] S. Bergman and M. Schiffer, *Kernel Functions and Elliptic Differential Equations in Mathematical Physics*, 1st ed. Dover Publications, 2005.

[18] O. D. Kellogg, *Foundations of Potential Theory*. Berlin, Heidelberg: Springer Berlin Heidelberg, 1967.

[19] W. Afzal and A. A. Masoud, "Harmonic potential-based communication-aware navigation of mobile agents in cluttered spaces," in *2016 IEEE 55th Conf. Decis. Control.* Las Vegas, Nevada, USA: IEEE, Dec. 2016, pp. 5146–5151.

[20] G. Dartmann, W. Afzal, X. Gong, and G. Ascheid, "Low complexity cooperative downlink beamforming in multiuser multicell networks," in *2010 IEEE 12th Int. Conf. Commun. Technol.*, vol. 49, no. 241. IEEE, Nov. 2010, pp. 717–721.

[21] G. Foschini and M. Gans, "On limits of wireless communications in a fading environment when using multiple antennas," *Wirel. Pers. Commun.*, vol. 6, no. 3, pp. 311–335, 1998.

[22] L. Hentilä, P. Kyösti, M. Käske, M. Narandzic, and M. Alatossava., "Matlab implementation of the winner phase ii channel model," 2007. [Online]. Available: http://www.ist-winner.org/phase_2_model.html